
This copy is for your personal, non-commercial use only.

If you wish to distribute this article to others, you can order high-quality copies for your colleagues, clients, or customers by [clicking here](#).

Permission to republish or repurpose articles or portions of articles can be obtained by following the guidelines [here](#).

The following resources related to this article are available online at www.sciencemag.org (this information is current as of August 19, 2014):

Updated information and services, including high-resolution figures, can be found in the online version of this article at:

<http://www.sciencemag.org/content/335/6074/1344.full.html>

Supporting Online Material can be found at:

<http://www.sciencemag.org/content/suppl/2012/03/14/335.6074.1344.DC1.html>

A list of selected additional articles on the Science Web sites **related to this article** can be found at:

<http://www.sciencemag.org/content/335/6074/1344.full.html#related>

This article **cites 55 articles**, 4 of which can be accessed free:

<http://www.sciencemag.org/content/335/6074/1344.full.html#ref-list-1>

This article has been **cited by** 10 articles hosted by HighWire Press; see:

<http://www.sciencemag.org/content/335/6074/1344.full.html#related-urls>

This article appears in the following **subject collections**:

Ecology

<http://www.sciencemag.org/cgi/collection/ecology>

quantum-chemical excited-state calculations of D-A pairs, we then inferred the nature of the electronic states at representative polymer-PCBM and polymer-polymer heterojunctions. Figure 4A features the charge density distribution as calculated in the lowest charge-transfer electronic excited state (CT_0) of a P3HT/PCBM heterojunction, and Fig. 4B shows the analogous situation for a higher-lying, strongly dipole coupled to CT_0 , excited state, CT_n , prepared by absorption of an IR photon from CT_0 . The P3HT-hole wave function, which was confined close to the PCBM electron in the CT_0 state, was more delocalized along the polymer backbone in the CT_n state, resulting in an increased average intermolecular electron-hole separation. The electron density on the fullerene was also changed upon the excitation to the CT_n state; however, as the electron is already delocalized on the fullerene molecule, this effect is not very pronounced. Nonetheless, current calculations cannot exclude further delocalization over more than one fullerene molecule when such molecules are available. Similar results were obtained for the P3HT/F8TBT interface (Fig. 4, C and D). Thus, at both heterojunctions, the strong IR transition from the CT_0 to the CT_n excited state, which correlates with the valence $\rightarrow n$ transition in a single P3HT chain, delocalizes the hole wave function along the donor chain and thereby promotes a larger intermolecular electron-hole separation. Although this transient delocalization is short-lived (subpicosecond), as measured by the all-optical technique in Fig. 4, B and D, it allows for charges to decouple and move apart at longer time scales (10 to 50 ps).

Although the general trend of delocalization of charge by optical excitation is observed for both modeled systems, the extent of delocalization is material dependent. Moving from F8TBT to PCBM increases the average electron-hole separation by 50%. This, in turn, induces even larger variations in CT-state binding energy and dissociation probability. The results of these variations are clearly seen in Figs. 1 and 3B. This difference in delocalization of charges causes OPV systems to demonstrate markedly different quantum efficiencies.

We propose that the driving energy for charge separation in organic photoconversion systems is the energy needed to reach delocalized band states, which are critical for long-range charge separation. Although the delocalized states are extremely short-lived (<1 ps), they enable charges to override the otherwise dominant Coulomb interaction. By contrast, large band offsets are not crucial for free-charge formation. Our results provide a new framework to understand charge generation in organic systems and outline the basis for the design of improved OPVs. In particular, those materials that support delocalized charge wave functions and have low reorganization energies due to structural rigidity and suppressed torsion relaxation should be targeted for the next generation of OPVs. This approach would mitigate the problem of polaron formation and allow

for efficient charge separation with minimal band offsets, greatly increasing the open-circuit voltage and efficiency of OPVs. The superior performance of fullerene-based OPVs is explained by meeting the outlined criteria, as is the performance of recently reported high-efficiency OPVs based on porphyrins (42, 43).

References and Notes

- R. E. Blankenship, *Molecular Mechanisms of Photosynthesis* (Blackwell Science, Oxford, 2002).
- T. M. Clarke, J. R. Durrant, *Chem. Rev.* **110**, 6736 (2010).
- G. Yu, J. Gao, J. C. Hummelen, F. Wudl, A. J. Heeger, *Science* **270**, 1789 (1995).
- M. M. Wienk et al., *Angew. Chem. Int. Ed.* **42**, 3371 (2003).
- Y. Kim et al., *Nat. Mater.* **5**, 197 (2006).
- J. Peet et al., *Nat. Mater.* **6**, 497 (2007).
- C. R. McNeill et al., *Adv. Funct. Mater.* **18**, 2309 (2008).
- R.-Q. Peng et al., *Nat. Mater.* **9**, 152 (2010).
- S. H. Park et al., *Nat. Photonics* **3**, 297 (2009).
- C. Deibel, T. Strobel, V. Dyakonov, *Adv. Mater. (Deerfield Beach Fla.)* **22**, 4097 (2010).
- S. Shoaee et al., *J. Am. Chem. Soc.* **132**, 12919 (2010).
- J.-L. Brédas, J. E. Norton, J. Cornil, V. Coropceanu, *Acc. Chem. Res.* **42**, 1691 (2009).
- T. Strobel, C. Deibel, V. Dyakonov, *Phys. Rev. Lett.* **105**, 26602 (2010).
- F. Etzold et al., *J. Am. Chem. Soc.* **133**, 9469 (2011).
- S. Gélinas et al., *J. Phys. Chem. C* **115**, 7114 (2011).
- A. C. Morteani, P. Sreearunothai, L. M. Herz, R. H. Friend, C. Silva, *Phys. Rev. Lett.* **92**, 247402 (2004).
- M. R. Jones, *Biochem. Soc. Trans.* **37**, 400 (2009).
- J. Piris et al., *J. Phys. Chem. C* **113**, 14500 (2009).
- S. A. Brazovskii, N. N. Kirova, *JETP Lett.* **33**, 4 (1981).
- D. K. Campbell, A. R. Bishop, K. Fesser, *Phys. Rev. B* **26**, 6862 (1982).
- X. Wei, Z. V. Vardeny, N. S. Sariciftci, A. J. Heeger, *Phys. Rev. B* **53**, 2187 (1996).
- R. Österbacka, C. P. An, X. M. Jiang, Z. V. Vardeny, *Science* **287**, 839 (2000).
- K. Vandewal, K. Tvingstedt, A. Gadisa, O. Inganäs, J. V. Manca, *Nat. Mater.* **8**, 904 (2009).
- J. G. Müller et al., *Phys. Rev. B* **72**, 195208 (2005).
- J. G. Müller, U. Lemmer, J. Feldmann, U. Scherf, *Phys. Rev. Lett.* **88**, 147401 (2002).
- S. V. Frolov, Z. Bao, M. Wohlgenannt, Z. V. Vardeny, *Phys. Rev. B* **65**, 205209 (2002).
- Materials and methods are available as supporting material on Science Online.
- M. A. Loi et al., *Adv. Funct. Mater.* **17**, 2111 (2007).
- D. Veldman et al., *J. Am. Chem. Soc.* **130**, 7721 (2008).
- R. D. Pensack, J. B. Asbury, *J. Am. Chem. Soc.* **131**, 15986 (2009).
- J. Lee et al., *J. Am. Chem. Soc.* **132**, 11878 (2010).
- V. I. Arkhipov, P. Heremans, H. Bassler, *Appl. Phys. Lett.* **82**, 4605 (2003).
- D. Veldman, S. C. J. Meskers, R. A. J. Janssen, *Adv. Funct. Mater.* **19**, 1939 (2009).
- A. A. Bakulin, D. Martynov, D. Y. Paraschuk, P. H. M. van Loosdrecht, M. S. Pshenichnikov, *Chem. Phys. Lett.* **482**, 99 (2009).
- R. A. Marsh, J. M. Hodgkiss, R. H. Friend, *Adv. Mater. (Deerfield Beach Fla.)* **22**, 3672 (2010).
- J. J. Benson-Smith et al., *Adv. Funct. Mater.* **17**, 451 (2007).
- K. Vandewal, K. Tvingstedt, A. Gadisa, O. Inganäs, J. V. Manca, *Phys. Rev. B* **81**, 125204 (2010).
- Y. S. Huang et al., *Nat. Mater.* **7**, 483 (2008).
- J. Holt, S. Singh, T. Drori, Y. Zhang, Z. V. Vardeny, *Phys. Rev. B* **79**, 195210 (2009).
- T. Drori, J. Holt, Z. V. Vardeny, *Phys. Rev. B* **82**, 075207 (2010).
- G. D. Scholes, *ACS Nano* **2**, 523 (2008).
- Y. Matsuo et al., *J. Am. Chem. Soc.* **131**, 16048 (2009).
- R. F. Service, *Science* **332**, 293 (2011).

Acknowledgments: We thank D. Y. Paraschuk, J. R. Durrant, J. Clark, and T. Strobel for useful discussions. A.A.B. acknowledges a Rubicon Grant from the Netherlands Organization for Scientific Research (NWO), cofinanced by a Marie Curie Cofund Action. A.R. thanks Corpus Christi College for a Research Fellowship. J.C. and D.B. are research fellows of the Belgian National Fund for Scientific Research (FNRS). This project was supported by the Engineering and Physical Sciences Research Council and the RTN SUPERIOR project.

Supporting Online Material

www.sciencemag.org/cgi/content/full/science.1217745/DC1
Materials and Methods
Figs. S1 to S9
Table S1
References (44–49)

12 December 2011; accepted 10 February 2012
Published online 23 February 2012;
10.1126/science.1217745

Climatic Niche Shifts Are Rare Among Terrestrial Plant Invaders

Blaise Petitpierre,¹ Christoph Kueffer,^{2,3} Olivier Broennimann,¹ Christophe Randin,⁴ Curtis Daehler,³ Antoine Guisan^{1*}

The assumption that climatic niche requirements of invasive species are conserved between their native and invaded ranges is key to predicting the risk of invasion. However, this assumption has been challenged recently by evidence of niche shifts in some species. Here, we report the first large-scale test of niche conservatism for 50 terrestrial plant invaders between Eurasia, North America, and Australia. We show that when analog climates are compared between regions, fewer than 15% of species have more than 10% of their invaded distribution outside their native climatic niche. These findings reveal that substantial niche shifts are rare in terrestrial plant invaders, providing support for an appropriate use of ecological niche models for the prediction of both biological invasions and responses to climate change.

Niche conservatism in space and time is a key assumption for predicting the impact of global change on biodiversity (1, 2). It is particularly important for the anticipation of biological invasions, which can cause severe dam-

age to biodiversity, economies, and human health (3). Niche conservatism implies that species tend to grow and survive under the same environmental conditions in native and invaded ranges (2). However, the generality of this assumption is

challenged by recent evidence suggesting that the climatic niche occupied by species may not be conserved between their native and invaded ranges, as documented by observed niche shifts for plants (4, 5), insects (6, 7), and fish (8). Yet, several of these studies have focused on a single species [e.g., (4, 6, 7)] or have used controversial niche overlap metrics [e.g., (5, 8); based on 26 and 18 species, respectively], making it difficult to assess the generality of this phenomenon among alien invasive species. Therefore, the question of whether niche shifts represent a prominent or unusual phenomenon among alien invasive species remains largely unresolved (9).

There are two major reasons why niche conservatism during biological invasion needs further investigation. First, anticipation is the most effective management strategy (10), and niche conservatism is a strong and necessary assumption to predict invasion risk for specific regions (1, 2). Ecological niche models (ENMs) (11, 12), the most commonly used predictive tool in this regard, are traditionally calibrated using native species distributions and then projected onto other continents to highlight areas susceptible to invasions (13). Second, detecting significant deviations from niche conservatism may highlight invasive species that are characterized by ecological (14, 15) or evolutionary changes (16, 17) during invasions, helping us understand when such changes are likely to occur, which is crucial in an era of rapid climate change.

When the niche of a species changes, its mean position (centroid) is likely to move within a multivariate environmental niche space. However, describing the shift of the centroid (4, 5, 7) falls short in helping to understand processes affecting the niche, because niche changes can affect both the position and shape of a niche. This is, for example, the case when species expand to new climates at one particular niche margin (1, 4) and only partially fill the niche (i.e., unfilling) at another (18) (e.g., due to dispersal limitation) (fig. S1). Assuming a species is at equilibrium in its native range (that is, it has colonized all suitable environments), expansion to climates that are new to the species but available in the native range should be considered unambiguously as niche shifts (fig. S1) (12); i.e., resulting from changes in biotic interactions or rapid evolution of the species (1). This conceptual approach to detecting niche shifts is important because analyses of empirical field data alone cannot determine whether the expansion to climates not available in the native range (that is, nonanalog climates) represents a true niche shift or the filling of a

preadapted niche. On the other hand, unfilling in the invaded range is more likely due to dispersal limitation, because biological invasions are recent and ongoing phenomena.

Niche changes due to unfilling have been considered niche shifts in previous studies (4–7), but our analyses (12) reveal that many of these reflect ongoing colonization instead, indicating that the species is likely to invade additional geographic

regions in the future (13). Thus, metrics of niche shift are very sensitive to the underlying statistical and conceptual assumptions, and a solid conceptual foundation for identifying ecologically meaningful and statistically significant niche changes has only recently been developed (12, 19–21).

Here, we disentangle and quantify the amount of niche overlap, niche expansion, and niche unfilling (see figs. S1 and S2) for 50 Holarctic

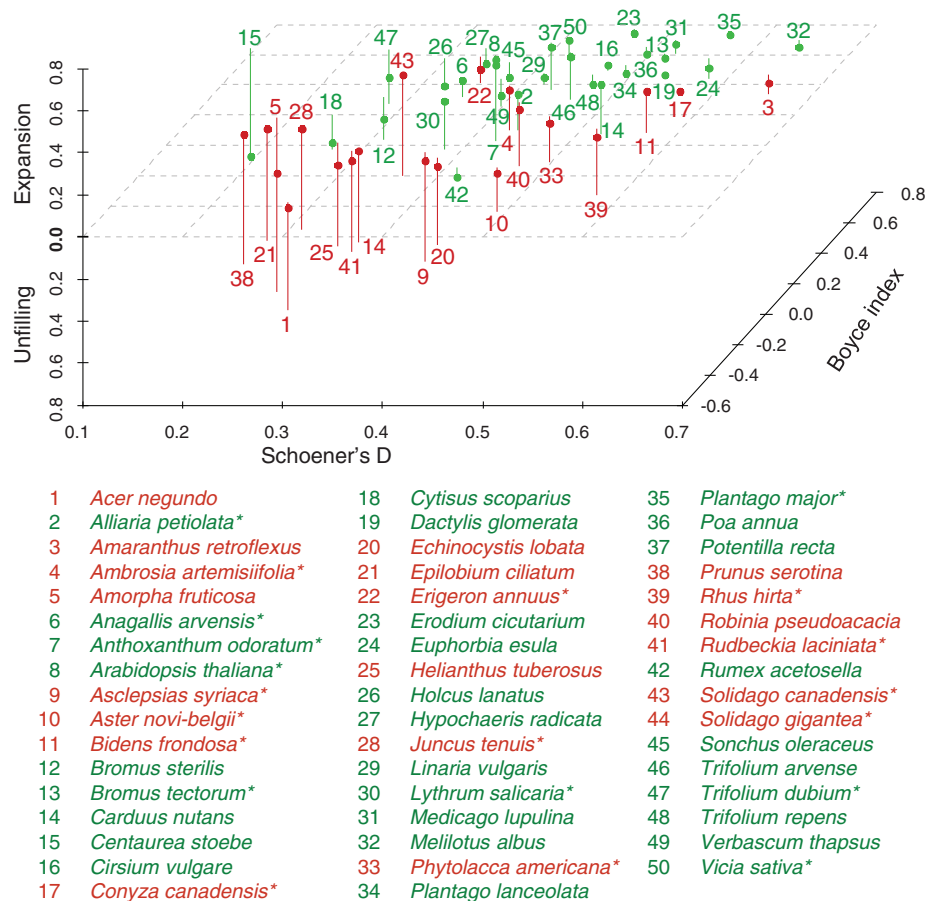
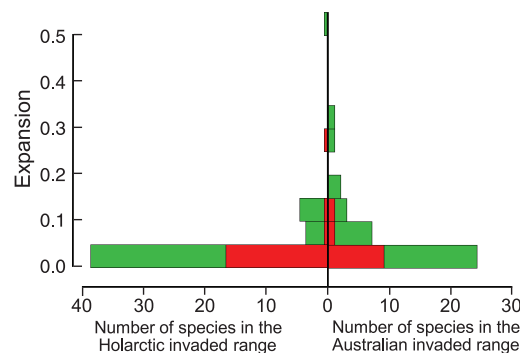


Fig. 1. Niche changes between native and invaded ranges in EU and NA. Vertical segments represent the magnitude of niche changes for each species. Extensions above and below the zero plane indicate expansion and unfilling, respectively. Intersections with the zero plane are shown with dots. Green (EU) and red (NA) colors indicate species origin. Niche-change indices are plotted over two niche-overlap indices, Schoener's D and the Boyce index evaluation of ENMs calibrated in the native range and projected onto analog climates in the invaded range. Asterisks denote species with a significant niche overlap between native and invaded range based on a similarity test.

Fig. 2. Expansion in Holarctic and Australian invaded ranges. The expansion index is analogous to the proportion of the invasive distribution in climate that is new to the species but available in the native range. NA and EU species origins are shown in red and green, respectively.



¹Department of Ecology and Evolution, University of Lausanne, Biophore Building, CH-1015 Lausanne, Switzerland. ²Institute of Integrative Biology, ETH Zürich, Universitätsstrasse 16, 8092 Zürich, Switzerland. ³Department of Botany, University of Hawaii at Manoa, 3190 Maile Way, Honolulu, HI 96822, USA. ⁴Institute of Botany, University of Basel, Schönbeinstrasse 6, 4056 Basel, Switzerland.

*To whom correspondence should be addressed. E-mail: antoine.guisan@unil.ch

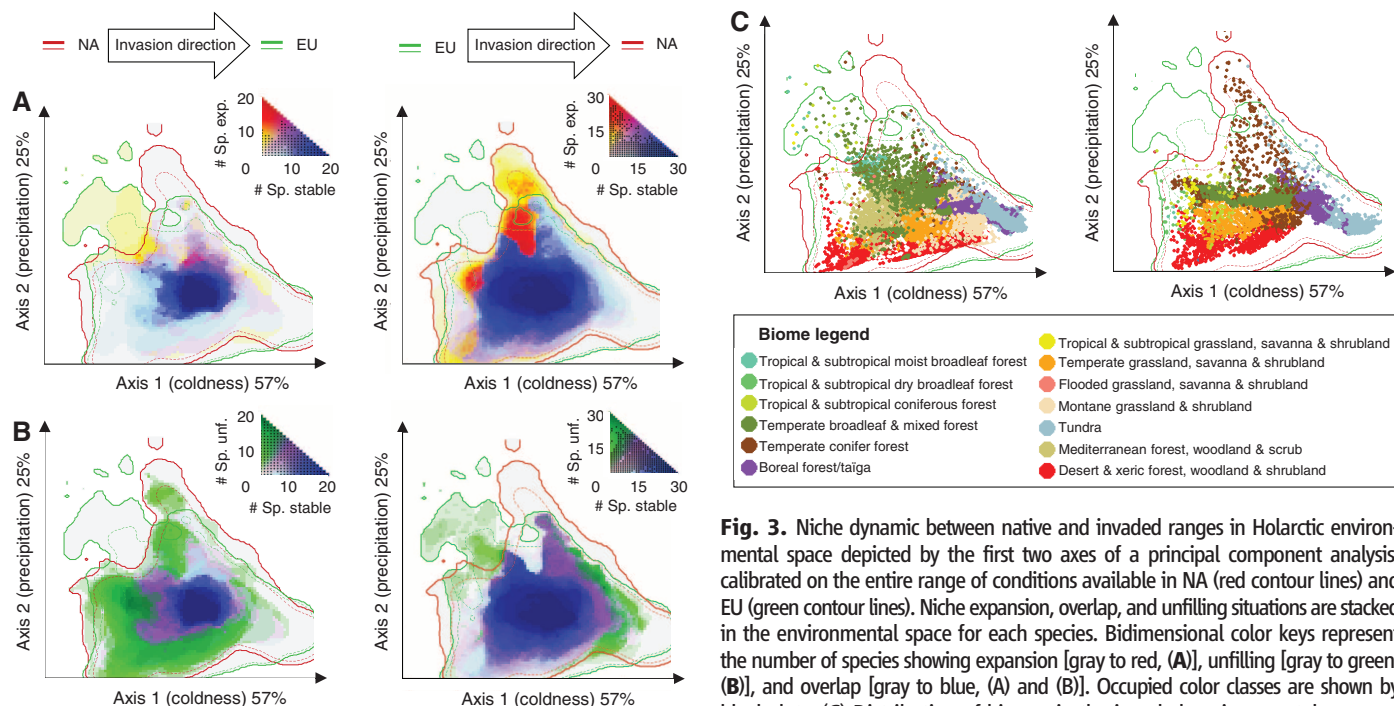


Fig. 3. Niche dynamic between native and invaded ranges in Holarctic environmental space depicted by the first two axes of a principal component analysis, calibrated on the entire range of conditions available in NA (red contour lines) and EU (green contour lines). Niche expansion, overlap, and unfilling situations are stacked in the environmental space for each species. Bidimensional color keys represent the number of species showing expansion [gray to red, (A)], unfilling [gray to green, (B)], and overlap [gray to blue, (A) and (B)]. Occupied color classes are shown by black dots. (C) Distribution of biomes in the invaded environmental space.

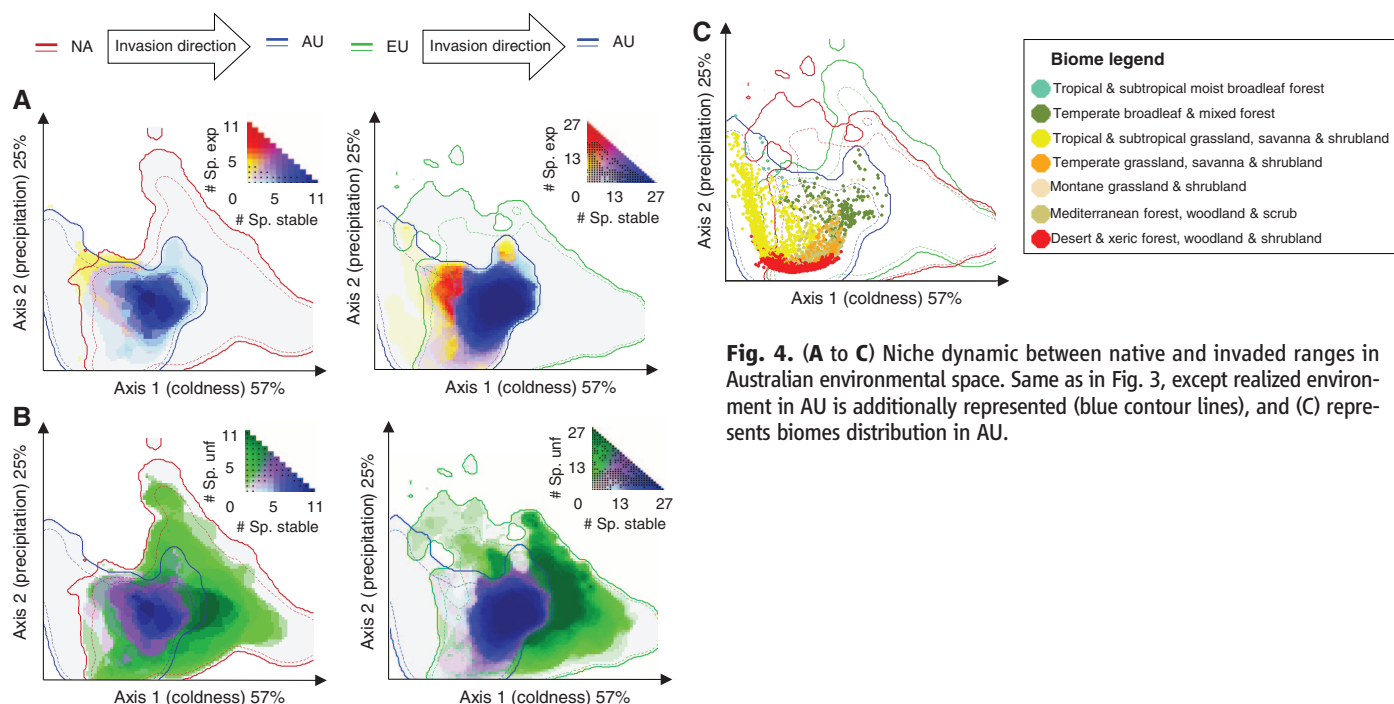


Fig. 4. (A to C) Niche dynamic between native and invaded ranges in Australian environmental space. Same as in Fig. 3, except realized environment in AU is additionally represented (blue contour lines), and (C) represents biomes distribution in AU.

terrestrial alien angiosperms (tables S1 and S2). Plants are appropriate for this test because their distributions are largely limited by climatic factors (22), a necessary condition to assess niche conservatism. Our sample includes many of the major plant invaders between North America (NA) and Eurasia (EU) and also many of the most anciently introduced EU species in NA. The reciprocal comparison of EU and NA invaders provides an important test of niche conservatism,

because EU and NA are the only pair of two large, separated land masses with a largely overlapping climate space and a long history of reciprocal anthropogenic exchanges of floras (23, 24). When available, the distribution of these species in Australia (AU) (table S3), where none is native, was used to provide additional, independent insights into patterns of niche filling when climatic availability, although partly overlapping, is overall very different from the native range. Geograph-

ical distributions (resolution = 0.5°, ~50 km) were projected onto climate space following a niche quantification framework correcting for species densities and climatic availability in both the native and invaded range (12, 21). This approach tests for niche conservatism and robustly quantifies the amount of niche overlap, expansion, and unfilling in the invaded range.

We find little evidence of niche expansion associated with the invasion of new regions. Our

results for the Holarctic reveal that, although levels of niche overlap among species vary between 17 and 64% (Fig. 1 and table S5), niche conservatism is observed for 46% (23) of species between the native and invaded range in EU and NA (similarity test with a significance level ≤ 0.05) (Fig. 1 and table S5). NA species show a higher propensity toward niche similarity (13 out of 20 species). In contrast to comparisons between EU and NA, niche similarity tests for AU are significant for all species (table S6), despite more pronounced climatic differences between AU and both EU and NA, respectively, than between EU and NA. This indicates that in AU, Holarctic invasive species remain in Holarctic climates and are rarely found in new climates. In other words, when considering the available climate in the invaded range, species colonize climatic conditions close to the ones colonized in their native range.

Further differentiating nonoverlap situations into cases of unfilling or expansion reveals that in the Holarctic, only 14% (7) of the studied species show more than 10% expansion, with only one outlier species—spotted knapweed (*Centaurea stoebe*)—showing >50% expansion (Figs. 1 and 2 and table S5). Previous studies also reported an important niche shift for this species (4), possibly caused by evolutionary (25) and/or ecological processes (15), notably through hybridization (4, 26) and enhanced competitive strength in the invaded range (27). There is also evidence of genetic admixing (repeated introductions or hybridization) and reduced impacts of competitors and enemies in many of the other studied species [e.g., (26, 28–30)], but these species did not show any major niche expansion, indicating that these mechanisms do not necessarily lead to niche expansion. Niche unfilling is a more widespread phenomenon with 48% (24) of species showing more than 10% of their native niche unfilled in the invasive range (Figs. 1 and 3). Patterns in AU confirm these Holarctic findings; i.e., niche expansion is uncommon compared to unfilling (Figs. 2 and 4, fig. S4, and table S6).

The biogeographical origin of the species provides further insights into niche comparisons between native and invaded ranges (Figs. 3 and 4). In general, EU species show less niche unfilling and more expansion in NA and AU than do NA species in EU and AU, thus mirroring biogeographical patterns of invasibility, which show higher invasion rates in NA compared with EU (31). Differences in the geographic arrangement of EU versus NA could account for the difference in niche unfilling. In particular, climate varies on a shorter distance along latitudinal gradients in NA than in EU and may allow more rapid expansion into different climates in NA (32). However, this does not explain why EU species also show less niche unfilling in AU than NA species. Biome conservatism, frequent across long evolutionary time scales (33) and highly expected in the case of invasive species (13), may further explain niche differences between areas differing in biome availability (Figs. 3 and 4). In NA and AU, EU species

expansions occur toward hotter and drier niche limits, corresponding in NA to the median climatic conditions of temperate coniferous forests, which are mostly absent in EU (Fig. 3). The lower prevalence of niche unfilling in EU species may relate to the longer history of weed selection in human-disturbed landscapes in Europe and earlier colonization paths from Europe to other continents (23, 24). However, when testing the effect of minimum residence time on niche expansion, overlap, unfilling, and total change magnitude, we found no significant effect (table S5), suggesting that other drivers, such as human-mediated propagule pressure, likely prevail. Movement of human settlements was far more important from EU toward NA and AU than the opposite (31), as shown by higher numbers of Eurasian invaders worldwide (24); this could explain less unfilling among EU species.

Our findings have implications for anticipating biological invasions, as they suggest that ENMs remain reasonable tools to predict invasions from the native range if study areas have comparable environments, at least with regard to the biologically relevant variables. This was indeed the rule in most of our species and thus is likely to also apply to many other terrestrial alien invasive plants. To illustrate this, we built ENMs for each species' native distribution. On average, the models reveal a fair transferability, with only a minority of poor predictions in the invaded range (eight NA species and two EU species) based on the Boyce index (B) (12). As expected, we found a positive correlation between B and the niche overlap D, as well as negative correlations between B and total niche changes (fig. S6). Interestingly, similar results are obtained when comparing niche metrics with ENM predictions calibrated on the analog climates between EU and NA or on the whole climate (fig. S7). The use of this approach to niche comparison (21) as a complement to ENMs thus remains important because it allows disentangling of disequilibrium situations, such as niche expansion or partial filling, in analog climates (Fig. 1).

Our findings that climatic niche shifts are rare among terrestrial plant invaders between their native and introduced ranges parallel results from a recent study showing that increases in species' abundance are rare between ranges (34). We found only a few plant invaders (such as spotted knapweed) that show an important proportion of their invaded range outside their native niche, possibly resulting from ecological and/or evolutionary changes, although we cannot exclude dispersal limitation in the native range as a possible contributing factor. Conversely, most reported niche differences are probably caused by partial filling of the native niche in the invaded range. Recognizing that some cases of true niche change do exist, further assessments should seek to understand strategies that have allowed these particular alien invasive species to expand their niches dramatically, with possible implications for biocontrol (35). Although our study focused on Holarctic plant

invaders, we included a wide range of plants, ranging from trees to herbs. It would be particularly interesting to use the same framework to test whether the same pattern is found in other organisms, especially in aquatic plants, as some of these are known to have a very large invaded range compared with their native one (36). Finally, our study specifically tested for niche change between geographic regions, but our general finding of niche conservatism also supports an important role for ENMs in assessments of species vulnerability to climate change over time (1).

References and Notes

- P. B. Pearman, A. Guisan, O. Broennimann, C. F. Randin, *Trends Ecol. Evol.* **23**, 149 (2008).
- J. J. Wiens, C. H. Graham, *Annu. Rev. Ecol. Syst.* **36**, 519 (2005).
- M. Vilà *et al.*, *Front. Ecol. Environ.* **8**, 135 (2010).
- O. Broennimann *et al.*, *Ecol. Lett.* **10**, 701 (2007).
- R. V. Gallagher, L. J. Beaumont, L. Hughes, M. R. Leishman, *J. Ecol.* **98**, 790 (2010).
- M. C. Fitzpatrick, J. F. Weltzin, N. J. Sanders, R. R. Dunn, *Glob. Ecol. Biogeogr.* **16**, 24 (2007).
- K. A. Medley, *Glob. Ecol. Biogeogr.* **19**, 122 (2010).
- C. Lauzeral *et al.*, *Glob. Ecol. Biogeogr.* **20**, 407 (2011).
- J. M. Alexander, P. J. Edwards, *Oikos* **119**, 1377 (2010).
- B. Leung *et al.*, *Proc. Biol. Sci.* **269**, 2407 (2002).
- A. Guisan, W. Thuiller, *Ecol. Lett.* **8**, 993 (2005).
- Materials and methods are available as supporting material on Science Online.
- W. Thuiller *et al.*, *Glob. Change Biol.* **11**, 2234 (2005).
- J. N. Klironomos, *Nature* **417**, 67 (2002).
- J. L. Hierro, D. Villarreal, O. Eren, J. M. Graham, R. M. Callaway, *Am. Nat.* **168**, 144 (2006).
- S. Lavergne, J. Molofsky, *Proc. Natl. Acad. Sci. U.S.A.* **104**, 3883 (2007).
- C.-Y. Xu *et al.*, *Ecol. Lett.* **13**, 32 (2010).
- E. Welk, *Ecol. Model.* **179**, 551 (2004).
- D. L. Warren, R. E. Glor, M. Turelli, *Evolution* **62**, 2868 (2008).
- L. Mandle *et al.*, *PLoS ONE* **5**, e15297 (2010).
- O. Broennimann *et al.*, *Glob. Ecol. Biogeogr.* **10.1111/j.1466-8238.2011.00698.x** (2011).
- F. I. Woodward, *Climate and Plant Distribution* (Cambridge Univ. Press, Cambridge, 1987).
- A. W. Crosby, *Ecological Imperialism: The Biological Expansion of Europe, 900–1900 (Studies in Environment and History)* (Cambridge Univ. Press, Cambridge, 1986).
- T. Seipel *et al.*, *Glob. Ecol. Biogeogr.* **21**, 236 (2012).
- U. A. Treier *et al.*, *Ecology* **90**, 1366 (2009).
- A. C. Blair, R. A. Hufbauer, *Evol. Appl.* **3**, 40 (2010).
- R. M. Callaway *et al.*, *Ecology* **92**, 2208 (2011).
- W. Durka, O. Bossdorf, D. Prati, H. Auge, *Mol. Ecol.* **14**, 1697 (2005).
- S. J. Novak, R. N. Mack, *Bioscience* **51**, 114 (2001).
- M. Pairon *et al.*, *Ann. Bot. (London)* **105**, 881 (2010).
- T. R. Seastedt, P. Pyšek, *Annu. Rev. Ecol. Syst.* **42**, 133 (2011).
- M. Rejmánek, *Austral. Ecol.* **25**, 497 (2000).
- M. D. Crisp *et al.*, *Nature* **458**, 754 (2009).
- J. Finn *et al.*, *Ecol. Lett.* **14**, 274 (2011).
- H. Müller-Schärer, U. Schaffner, T. Steinger, *Trends Ecol. Evol.* **19**, 417 (2004).
- I. W. Forno, *Aquat. Bot.* **17**, 71 (1983).

Acknowledgments: We thank R. Engler, E. Schumacher, and C. Angelo for contributing to the compilation of the data and J. Alexander, H. Possingham, L. Pellissier, and S. M. Gray for comments on the manuscript. A.G., O.B., and B.P. received main support from the National Center for Competence in Research (Plant Survival). C.D. and C.K. received support from the USDA National Institute of Food and Agriculture,

Biology of Weedy and Invasive Species Program grant no. 2006-35320-17360. The climatic data used in this study are available online, and the species data used in this study were assembled from multiple sources with various release politics. All data sources are described in the SOM.

Supporting Online Material
www.sciencemag.org/cgi/content/full/335/6074/1344/DC1
Materials and Methods
SOM Text
Figs. S1 to S10

Tables S1 to S9
References (37–65)

28 October 2011; accepted 6 February 2012
10.1126/science.1215933

The Path from β -Carotene to Carlactone, a Strigolactone-Like Plant Hormone

Adrian Alder,¹ Muhammad Jamil,² Mattia Marzorati,³ Mark Bruno,¹ Martina Vermathen,³ Peter Bigler,³ Sandro Ghisla,⁴ Harro Bouwmeester,^{2,5} Peter Beyer,^{1,6} Salim Al-Babili^{1,6*}

Strigolactones, phytohormones with diverse signaling activities, have a common structure consisting of two lactones connected by an enol-ether bridge. Strigolactones derive from carotenoids via a pathway involving the carotenoid cleavage dioxygenases 7 and 8 (CCD7 and CCD8) and the iron-binding protein D27. We show that D27 is a β -carotene isomerase that converts all-*trans*- β -carotene into 9-*cis*- β -carotene, which is cleaved by CCD7 into a 9-*cis*-configured aldehyde. CCD8 incorporates three oxygens into 9-*cis*- β -apo-10'-carotenal and performs molecular rearrangement, linking carotenoids with strigolactones and producing carlactone, a compound with strigolactone-like biological activities. Knowledge of the structure of carlactone will be crucial for understanding the biology of strigolactones and may have applications in combating parasitic weeds.

The biosynthetic carotenoid pathway provides precursors for smaller, physiologically important compounds such as the plant hormone abscisic acid (1), the vertebrate morphogen retinoic acid (2), and the fungal pheromone trisporic acid (3), which originate from oxidative cleavage of C-C double bonds in carotenoid backbones (4–7). The derivative compounds, named apocarotenoids (see fig. S1 for nomenclature and structures), may undergo structural modifications concealing their origin. Strigolactones, a prominent example of such compounds, are a group of metabolites with a common C₁₉ structure (e.g., 5-deoxystrigol, Fig. 1A) consisting of a tricyclic lactone (A, B, and C rings) connected via an enol ether bridge to a second lactone (D ring) (8). Several lines of evidence demonstrate that strigolactones derive from carotenoids. A putative biosynthetic pathway has been proposed, leading from a C₁₅ apocarotenal to the ABC C₁₄ skeleton, which is then coupled to a butenolide group (D ring) of unknown origin (9).

Released by plant roots, strigolactones trigger seed germination of root parasitic weeds such as witchweeds (*Striga* spp.) (10) and can induce hyphal branching in arbuscular mycorrhizal fungi, an essential step in establishing the symbiosis

(11). In plants, strigolactones inhibit tillering and shoot branching. High tillering (more branching) is observed in plant mutants disrupted in *Carotenoid Cleavage Dioxygenase 7* (CCD7) and CCD8, in *Dwarf27* (D27) encoding an iron-binding polypeptide with unknown catalytic properties, or in a cytochrome P450 gene represented by *More Axillary Growth 1* (MAX1) from

Arabidopsis thaliana (8, 12–17). The application of the synthetic strigolactone GR24 restored the wild-type tillering/branching phenotype of these mutants, suggesting the involvement of CCD7, CCD8, D27, and MAX1 in strigolactone biosynthesis (8, 12–17).

CCDs are nonheme iron enzymes that cut C-C double bonds by incorporating a dioxygen, yielding carbonyl products (4–7). It was supposed that CCD7 from *Arabidopsis* (AtCCD7) cleaves all-*trans*- β -carotene (C₄₀; Fig. 1A) into all-*trans*- β -apo-10'-carotenal (C₂₇) that is then further shortened by AtCCD8 to the C₁₈ ketone β -apo-13-carotenone (Fig. 1B) (18), a biologically active compound affecting the growth of root hairs in plants (19). The sequential activity of the two cleavage enzymes was deduced from the coexpression of AtCCD7 and AtCCD8 in *Escherichia coli* strains accumulating all-*trans*- β -carotene (18) and confirmed by in vitro studies showing the formation of β -apo-13-carotenone from all-*trans*- β -apo-10'-carotenal by CCD8 enzymes from different plant species (20). However, the structure of β -apo-13-carotenone has little in common with that of strigolactones, and treatment of rice *ccd8* mutant with this compound did not restore the wild-type tillering phenotype (fig. S2).

We used an in vitro approach to investigate the activities of CCD7 and CCD8 from *Arabidopsis*,

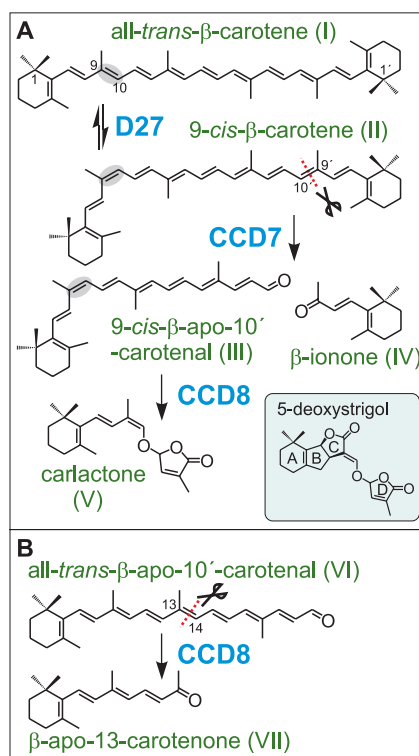


Fig. 1. The pathway to carlactone. **(A)** D27 catalyzes the isomerization of the C9-C10 double bond (shaded) in all-*trans*- β -carotene (I; C₄₀), leading to 9-*cis*- β -carotene (II) that is cleaved by CCD7 at the C9', C10' position into 9-*cis*- β -apo-10'-carotenal (C₂₇; III) and β -ionone (C₁₃; IV). A single enzyme, CCD8, converts III to carlactone (V) that already contains the D ring and the enol ether bridge of strigolactones such as 5-deoxystrigol (inset). **(B)** CCD8 also catalyzes a known CCD reaction by converting all-*trans*- β -apo-10'-carotenal into β -apo-13-carotenone. However, this reaction is slower than that with the *cis* isomer by about a factor of 10.

¹Faculty of Biology, University of Freiburg, 79104 Freiburg, Germany. ²Laboratory of Plant Physiology, Wageningen University, 6700 AR Wageningen, Netherlands. ³Department of Chemistry and Biochemistry, University of Bern, 3012 Bern, Switzerland. ⁴Department of Biology, University of Konstanz, 78457 Konstanz, Germany. ⁵Centre for Biosystems Genomics, 6700 AR Wageningen, Netherlands. ⁶Centre for Biological Signalling Studies (Bioss), 79104 Freiburg, Germany.

*To whom correspondence should be addressed. E-mail: salim.albabili@biologie.uni-freiburg.de